Characteristics of Sn–Cu Solder Bump Formed by Electroplating for Flip Chip

Seok Won Jung, Jae Pil Jung, and Y. (Norman) Zhou

***Abstract*—Sn–Cu near eutectic solder bump was fabricated by electroplating for flip-chip, and its electroplating and bump characteristics were studied. A Si-wafer was used as a substrate and the under bump metallization (UBM) comprised 400 nm of Al, 300 nm of Cu, 400 nm of Ni, and 20 nm of Au sequentially from bottom to the top of the metallization. The electrolyte for plating Sn–Cu solder consisted of Sn^{+2} (concentration of 30 g/L) and Cu^{+2} (0.3 g/L) solutions with methasulfonic acid and deionized water. The experimental results showed that the plating ratio of the Sn–Cu increased from 0.25 to 2.7 μ/min with increasing current density from 1 to 8 A/dm^2. In this range of current density, the plated Sn–Cu maintained its composition nearly constant level as Sn-(0.9$\sim$1.4)wt% Cu. The solder bump of typical mushroom shape with 120-μm stem diameter and 75-μm height was formed by plating at 5 A/dm^2 for 2 h. The mushroom bump changed its shape to the hemispherical type of 140-μm diameter by air reflow on a hot plate at 260 °C. The homogeneity of element distribution in the solder bump was examined, and Sn content in the mushroom bump appears to be uneven changed to more uniform after the air reflow. The highest shear bond strength of the Sn–Cu hemispherical bump showed 113 gf by reflowing at 260 °C for 10 s.**

***Index Terms*—Electroplating, flip-chip, lead-free solder, Sn–Cu eutectic, solder bump.**

I. Introduction

IN THE electronic packaging industry, high-integrity and lead-free solder for electronic devices have been two important issues. In the field of lead-free solder, Sn–Ag–Cu alloys almost dropped in because of its good reliability in mechanical properties and sufficient supply [1], [2].

Related to integrity, a flip-chip technology can secure higher pin counts than wire bonding and improve electrical performance [3]. A bumping technology on a Si-wafer is an important issue to obtain high productivity of the flip-chip. Several methods for solder bumping have been introduced, such as paste [3], ball [4], electroplating [5], and vapor deposition [6].

Among them, the paste bumping method has a risk of pollution by solder flux even though it has high productivity. In addition, it may have a difficulty to achieve height uniformity of the bump due to misprinting. The vapor deposition method is regarded as a clean one, but it has a demerit of higher price due to the vacuum process and of very careful control [6]. The ball bumping method can be performed by fluxed or nonfluxed processes such as ultrasonic [7] or plasma [4], but it also has disadvantages of relatively big size, higher price, and troublesome mounting of a tiny ball.

On the other hand, the bumping by electroplating has lower price, mass productivity, and ability to fabricate tiny bumps due to a precise patterning bya photo technique. However, the electroplating method is apt to get an inconsistent composition of a solder bump. This problem can be improved by controlling current density [8] and by additives in electroplating solution [9].

In Pb-free solders, Sn–Ag–Cu, a ternary alloy, is relatively hard to get a reliable composition by electroplating. Since the standard equilibrium potentials of Ag and Cu are much more positive than that of Sn, the deposition of Ag and Cu should be controlled to get a eutectic composition [10]. In the case of the Sn–Ag eutectic alloy, some studies are reported about electroplating [5], [11], but its disadvantage is high price. Besides, Sn–Ag–Cu [12] and Sn–Ag [13] eutectic alloys have much higher solubility of Cu than Sn–Pb eutectic. Namely, the saturation solubility of Cu in molten solder is 1.54% (at 260 °C), around 3% (at 254 °C), and 0.18% (at 220 °C) for the eutectic Sn–Ag–Cu, Sn–Ag and Sn–Pb, respectively [12], [13]. Thus, the eutectic Sn–Ag–Cu and Sn–Ag can cause excessive consumption of the Cu pad in flip-chip during soldering.

On the other hand, though the Sn–Cu eutectic alloy has a higher melting point (227 °C) compared to Sn–Ag–Cu alloy (217 °C), it has lower price and an easiness to control composition during electroplating. Besides, the Sn–Cu eutectic alloy has comparable wettability compared to the Sn–Ag eutectic solder [14]. Some studies on the Sn–Cu electroplating have been reported [10], [15], [16]. Fukuda *et al.* [10] suggested the mechanism of an additive polyoxythylene laurylether, (POELE) effect on Sn–Cu deposition to get smooth and homogeneous alloy film. In their other paper [15], it was reported they got a eutectic Sn–Cu deposition by addition of the POELE. Arai *et al.* [16] also studied about the effect of additives, polyethylene glycol and formaldehyde, on the composition of electrodeposits and surface morphology. However, they mainly investigated about the additives and the films of Sn–Cu deposits, and, hence, the bump formation process and bump joint properties such as bond strength were not described in their papers.

Bump shape and its joint properties are important for industrial application of the Sn–Cu bump. Thus, in this study, the fabrication and characteristics of the Sn–Cu bump on the Si-wafer by the electroplating process were examined. In addition, the joint strength of the Sn–Cu bump after reflow was investigated

Manuscript received May 28, 2004; revised May 13, 2005. This work was supported by the Korea Science and Engineering Foundation under Grant R01-2004-000-10572-0.

S. W. Jung and J. P. Jung are with the Department of Material Science and Engineering, University of Seoul, 130-740 Seoul, Korea (e-mail: jpjung@uos.ac.kr).

Y. Zhou is with the Department of Mechanical Engineering, University of Waterloo, Waterloo, ON N2L 3G1, Canada.

Digital Object Identifier 10.1109/TEPM.2005.863266

1521-334X/$20.00 © 2006 IEEE

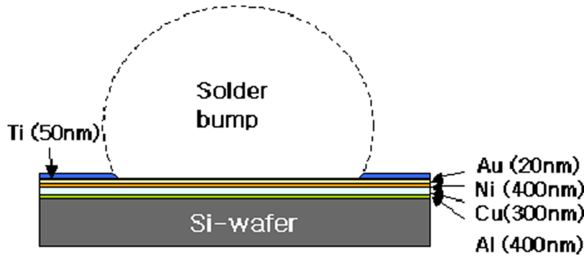

Fig. 1. Schematic illustration of UBM layers. (Color version available online at http://ieeexplore.ieee.org.)

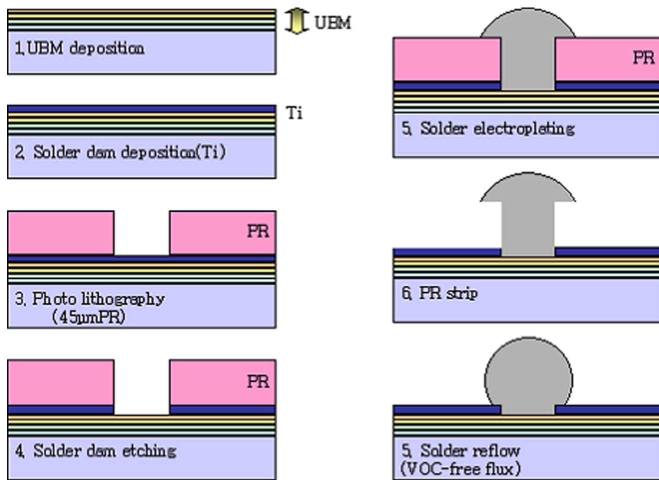

Fig. 2. Explanation of bumping procedure by electroplating. (a) Sn–Cu. (b) Sn–Pb [5]. (Color version available online at http://ieeexplore.ieee.org.)

and compared to our previous results of Sn–Ag and Sn–Pb electroplated bumps [5].

II. Experimental

An under bump metallization (UBM)-coated Si-wafer was prepared as a substrate for a soldering specimen. The UBM consisted of Al/Cu/Ni/Au layers from bottom to top of the metallization sequentially, and their thicknesses were 20 nm/400 nm/300 nm/400 nm, respectively (Fig. 1). The UBM layers were deposited by an electron-gun evaporator. The area of the UBM for solder bumping was 110 μm in diameter with 250-μm pitch, and the remaining UBM was masked by a Ti-layer to serve as a dam against molten solder.

With the purpose of making a pattern for the electrodeposition of solder bumps, a positive photoresist (PR) was spin-coated by 2500 r/min on the UBM. Thickness of the PR was 45 μm, and it was heated at 100 °C. Then, the PR was exposed to a light and developed. The Ti-layer for the solder dam was also etched away by buffered oxide etcher (BOE). Through this work, the mould sized at 110-μm diameter and 250-μm pitch was prepared. On the mould, Sn–Cu solder was electroplated to form a bump with mushroom shape. The experimental procedure to make solder bumps is illustrated in Fig. 2.

An electrolytic solution produced by the MacDiarmid Co. was used for this study. The electrolyte composed of Sn^{+2} (concentration of 30 g/L) and Cu^{+2} (0.3 g/L) solutions with the addition of methasulfonic acid and deionized water. The Si-substrate to be electroplated was cleaned by ultrasonic in acetone and followed by deionized water cleaning.

In the electrolytic bath, platinum-coated titanium mesh was used for the anode, and the cathode was UBM-coated substrate with 20 × 20 mm size. Electroplating was performed at 20 °C to avoid loss of volatile substances and the oxidation of stannous tin. The bath used direct current (dc) electrolysis, and the distance between cathode and anode was 27 mm. The solution was agitated by a magnetic stirrer with a rotating speed of 240 r/min. The cathode current density was changed in the range of 1–8 A/dm^2, and the plating time was extended to 2 h.

After plating Sn–Cu on the substrate, the PR-mould was stripped and as a result mushroom shaped bump was obtained. The uniformity of the plated solder bumps was measured by an alpha step profiler. Then, the plated bumps coated with volatile organic compound (VOC)-free flux were reflowed on a hot plate in air. The reflow temperature was 260 °C which was about 30 °C higher than its melting point, 227 °C.

The uniformity of element distribution in the bumps as electroplated and as in the reflowed state was estimated by an energy probe microanalyzer (EPMA). The bump shape was examined by scanning electron microscopy (SEM). The shear test specimen with hemispherical bumps was prepared by reflowing the mushroom bump for 5, 10, 30 s, and the bond strength was measured by a microshear tester. The clearance between the shearing tip and the UBM was 5 μm, and shearing speed was 200 μm/s.

III. Results and Discussion

A. Electroplating of Solder

Fig. 3 shows polarization curves with current density during electroplating solders on Si-wafer. The polarization curve of Sn–Pb eutectic [5] was given for comparison. In the curve of Sn–Pb [Fig. 3(b)], a reduction reaction of dissolved oxygen occurred in the region ⟨A⟩. In the region ⟨B⟩, both tin and lead ions were plated on the cathode substrate together, because the standard electrode potential of tin and lead are similar. The region ⟨C⟩ indicates where hydrogen was generating.

On the other hand, the polarization curve of the Sn–Pb [Fig. 3(a)] is a little different from that of Sn–Pb. The standard electrode potential of copper is 0.337 V, and it is much greater than that of tin (−0.376 V). This causes copper reduced on the cathode prior to tin. Moreover, the limiting current density (i_L) seems not to appear on the Sn–Cu polarization curve. The limiting current density means that the cathode current density stays constant even increasing electric potential. In this region, the ions to be plated are depleted around the cathode, and the plating rate does not increase.

In the curve of Sn–Pb, however, the limiting current density appeared around 4–5 A/dm^2. Kim *et al.* [17] reported the limiting current of Sn-20%Pb alloy appeared around 3 A/dm^2, and this looks not so different from our result.

The plating rate of Sn–Cu with current density was compared with Sn–Ag and Sn–Pb in Fig. 4. Generally, the plating rate with current density can be guessed as (1), which was derived from Faraday's law [18].

$$x(\mu\text{m})/t(\text{min}) = E_c i \varepsilon / 60\rho \quad (1)$$

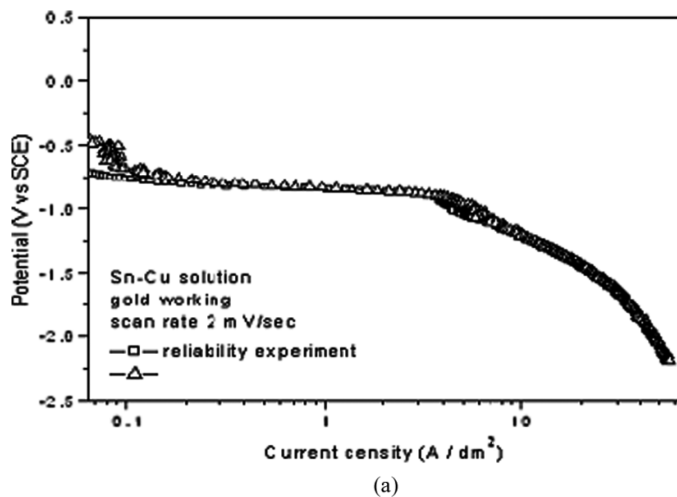

(a)

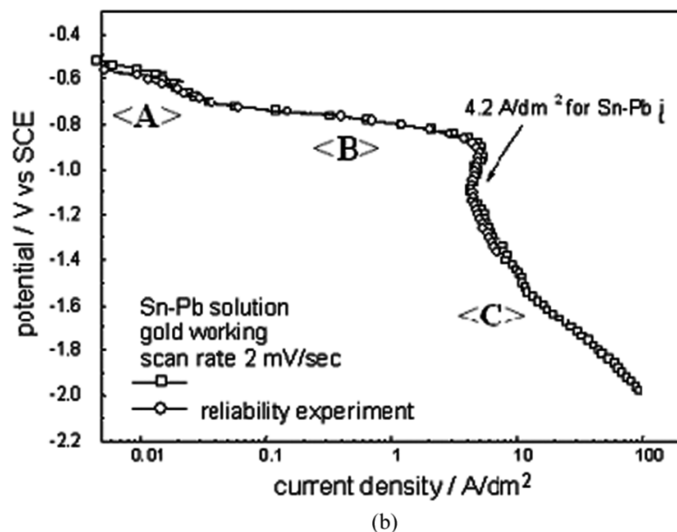

(b)

Fig. 3. Polarization curves during Sn–Cu and Sn–Pb electroplating. (a) Sn–Cu. (b) Sn–Pb [5].

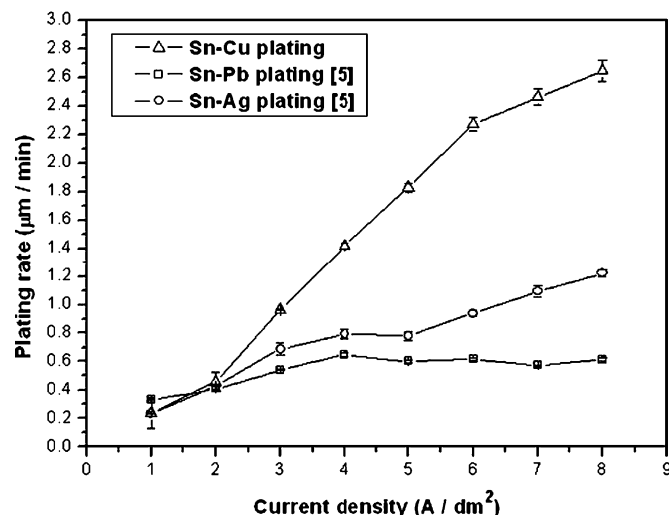

Fig. 4. Electroplating rate of solders with current density.

where x is thickness of deposit, t plating time, E_c electrochemical equivalent of deposit, i current density, ε cathodic current efficiency, and ρ density of deposit.

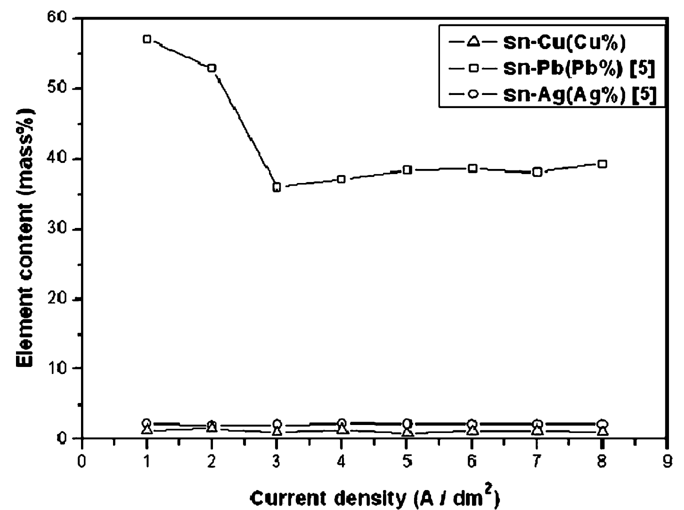

Fig. 5. Contents of element in the electroplated solders with current density.

From (1), it is found that thickness of electroplated element (x) and its plating rate (x/t) are proportional to the current density (i). The limiting current density also has a weighty effect on the suppressing of plating rate as mentioned previously. In Fig. 4, the plating rates of solders show the tendency to increase with current density as (1), except Sn–Pb in special range. The plating rate of Sn–Cu is higher than others, namely, it increased 10 times (from 0.25 to 2.7 $\mu\mathrm{m/min}$) by raising current density from 1 to 8 A/dm^2. In the case of Sn–Pb, however, the rate increased only to around 4 A/dm^2. After that, in the range of 4–8 A/dm^2, the plating rate keeps constant, and the reason can be explained as the limiting current density as shown in Fig. 3. That means in Sn–Pb, the limiting current density which suppresses plating rate starts around 4 A/dm^2.

The plating thickness of Sn–Cu increased with plating time, and the value was 1.5, 3.3, and 5.9 μm for 5, 10, and 15 min, respectively, at the current density of 2 A/dm^2. This result corresponds to the (1), where the thickness (x) is proportional to the plating time (t). In the case of Sn–Ag, it had a similar tendency with Sn–Cu, as the thickness was 2.6, 4.3, and 6.1 μm for 5, 10, and 15 min, respectively, at the same current density [5].

In the electroplating procedure, it is important to keep a consistent composition on the plated layer because it is related with uniform deposits. The chemical composition can be changed by current density, additives, and agitation [5], [19], [20]. A variation of chemical composition on the plated layer with current density is given in Fig. 5. In the range of 1–8 A/dm^2, the Sn–Cu layer had a composition range between 0.9 and 1.4 wt% Cu, while the proportion of copper to tin in the electrolyte was 1% (concentration of Sn^{+2} and Cu^{+2} was 30 and 0.3 g/L, respectively).

The consistence of Sn–Cu composition with current density looks similar to the result of Sn–Ag in Fig. 5. Actually, the composition variation with current density was reported to have a relationship with the electroplating type like a regular or an irregular [21]. That means in the regular plating type the plating process can be under diffusion control, i.e., under mass-transport control in solution. On the other hand, the irregular plating type is controlled by cathode potential, and it is not influenced

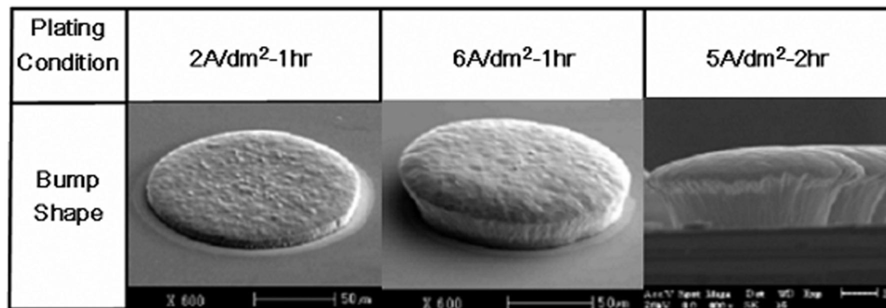

Fig. 6. Shapes of electroplated Sn–Cu solder bumps according to the plating condition.

by the current density. From Fig. 5, composition of Sn–Cu looks not sensitive to the current density, and it seems to have a characteristic of the irregular type. Even though, its electroplating type is not clear because the Cu content is quite as low as 0.7 wt% and, hence, analysis reliability cannot be high enough.

Meanwhile, in the case of Sn–Pb, Pb content of 57% at 1 A/dm^2 decreased greatly in the range of 2–3 A/dm^2, and reached to the constant values around 35–40 wt% after limiting current density of 4 A/dm^2. Carano [19] reported that tin content in the Sn–Pb deposit increases with increasing cathode current density. Thus, the result of Fig. 5 showed agreement with his result in the range of 1–3 A/dm^2. However, Sn content in the plated layer is also affected by the additives. In reality, the additives and current density are interlinked, and their effects are recommended to consider together.

B. Fabrication and Evaluation of Solder Bumps

Sn–Cu solder bumps were fabricated by changing electroplating condition, and some of the results were shown in Fig. 6. A bump with less than 10 μm height was produced [Fig. 6(a)] when a plating current density was as low as 2 A/dm^2 and the plating time was 1 h. However, a higher bump can be expected to form through current density enhancement, because from Fig. 4, plating rate is increased by increasing current density. Increasing current density to 5 or 6 A/dm^2 gave better bump shape as in Fig. 6(b) and (c). In the condition of 5 A/dm^2 and 2-h plating, the mushroom bump had a 120-μm column diameter and 75-μm height. When the current density and plating time exceeded this plating condition, the bumps connected with neighbors. Contrarily, when the condition did not reach this condition, sometimes the bump height was lower than the mould height. Since this result was the closest to our expectation, 5 A/dm^2—2 h was determined as the optimal plating condition to make mushroom and hemispherical bumps.

Fig. 7 gives the arrays of mushroom bumps formed on Si-wafer by the optimal plating condition, and they show uniform shape and size. The average size was 120-μm column diameter and 75-μm bump height.

The distribution of the elements in the mushroom bump was analyzed by EPMA, and the result is given in Fig. 8. In the figure, Sn has a concentration difference according to a position, but Cu shows just little difference. Phosphor (P), which comes from the electrolyte, shows negligible concentration difference due to its infinitesimal content in the bump. Concentration difference in the bump can come from the localized chemical environment in the bath, local electrodeposition current, etc. [22]. Besides, the intermetallic compound of Cu_6Sn_5 was found by X-ray dispersive (XRD) analysis from the Sn–Ag–Cu eutectic electrodepostion [15], and it can cause local concentration difference of Cu. From these reports, the nonuniformity of Cu in Fig. 8 has a possibility to occur from similar reasons.

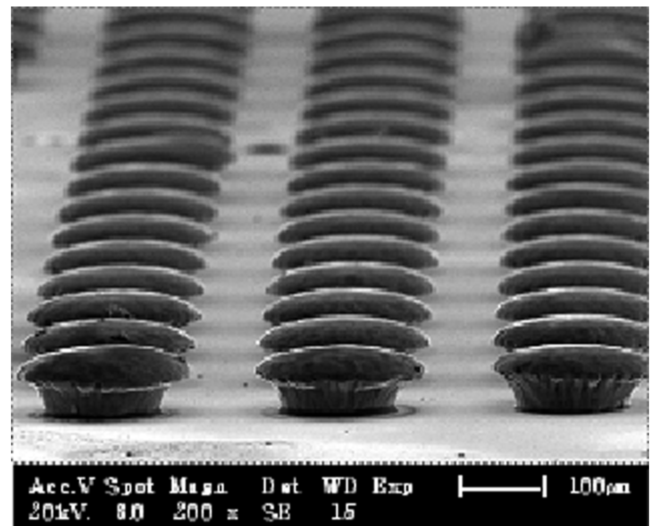

Fig. 7. Sn–Cu solder bumps formed on a Si-wafer by electroplating.

In Fig. 9, hemispherical bumps were given which were produced by reflowing mushroom bumps on a hot plate. The hemispherical bumps had a uniform shape with 140-μm diameter and 250-μm pitch, and it was confirmed the electroplating process gave a satisfying result for bumping. Element distribution in the hemispherical bump was analyzed by EPMA, and the result was given in Fig. 10. Sn, Cu, and P were estimated to have almost even distributions on the bump, and the nonuniformity of Sn from Fig. 8 decreased to a higher degree. The reason is believed that during the air reflow the mushroom bump melted, and in the liquid state the local concentration difference became homogenized by rapid diffusion. However, it is found that Sn concentrated more on the local area around the left bottom of the bump. It is not clear why this area was not homogenized in melt state. The reason can just be guessed that during solidification intermetallic compound (IMC) of Sn–Cu could be formed, and diffusion time might not be enough to homogenize during cooling.

To estimate the soundness of the hemispherical bump, its bond shear strength was evaluated (Fig. 11). The shear strength

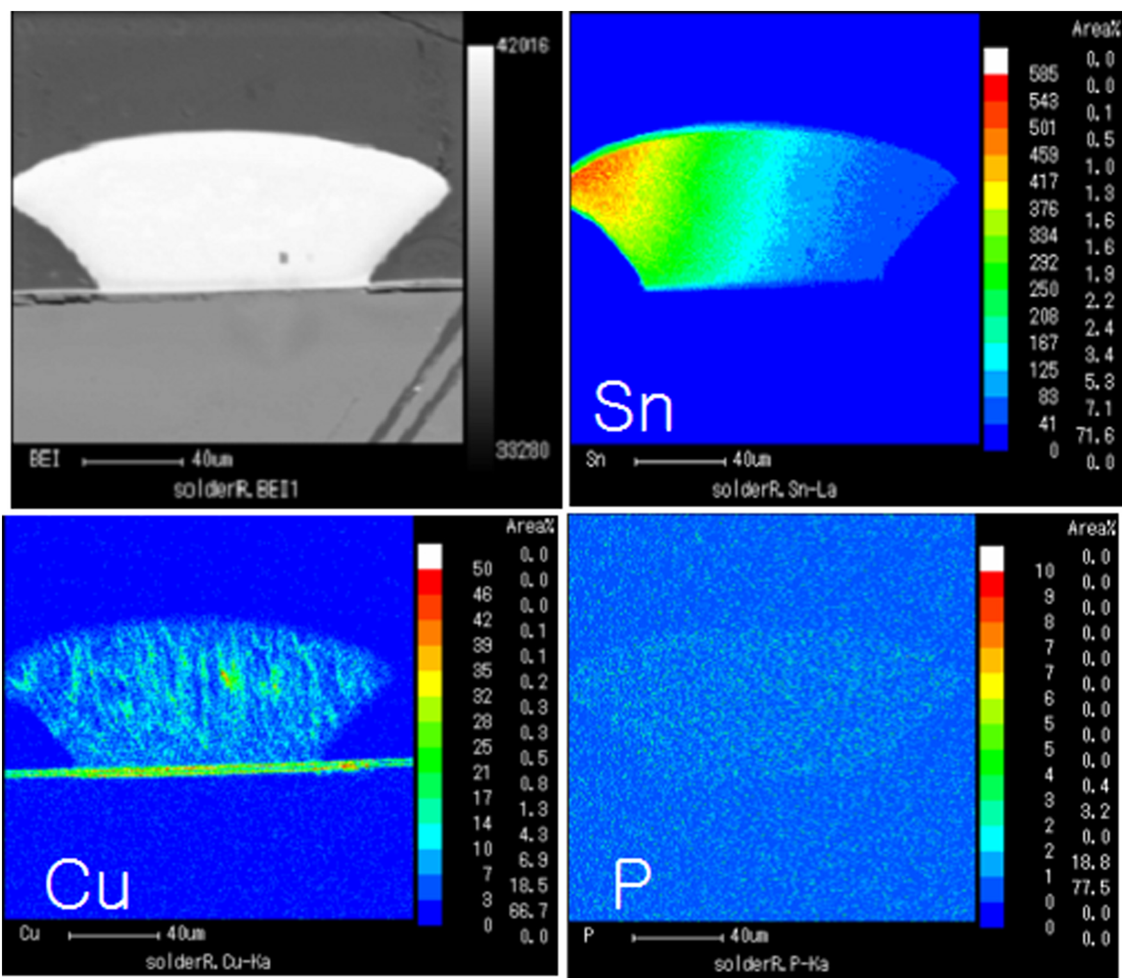

Fig. 8. Analysis of element distribution by EPMA mapping on the electroplated Sn–Cu solder bump. (Color version available online at http://ieeexplore.ieee.org.)

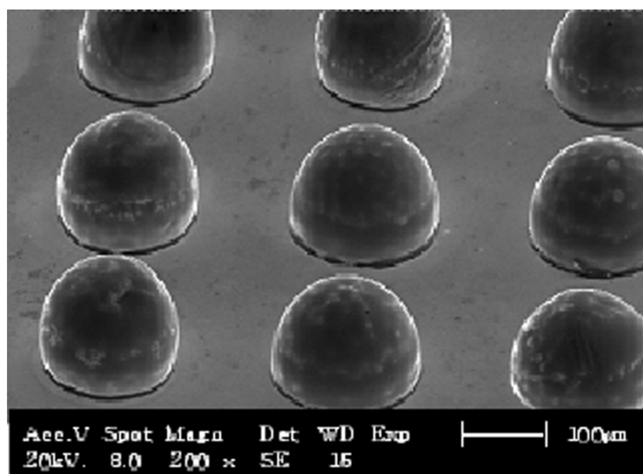

Fig. 9. Appearance of Sn–Cu solder bumps by air reflow with VOC-free flux.

in Sn–Cu increased with reflow time to 10 s, and showed the highest value of 113 gf. The strength of the Sn–Cu was a little lower than that of Sn–Ag, but higher than Sn–Pb. The bond strength was also compared with that of other bumping process. The bond strength in Fig. 11 was higher than the bump formed by ultrasonic which showed 40 gf in Sn-3.5 Ag with the ball size of 100-μm diameter [7]. However, the electroplated bump has similar strength compared to the result from air reflow with flux, 120 gf in Sn-3.5 Ag, where the bump was prepared by solder ball with 100-μm diameter [4]. Therefore, from these comparisons, the bump fabricated by electroplating was estimated to have an acceptable strength.

IV. Conclusion

Sn–Cu near eutectic solder was electroplated on the UBM-coated Si-wafer as a lead-free candidate for flip-chip. The UBM consisted of Au–Ni–Cu–Al layers, and their thicknesses were 20 nm/400 nm/300 nm/400 nm, respectively. The Sn–Cu solder bump of a mushroom shape was formed by electroplating, and it was changed to a hemispherical shape by air reflow. Characteristics of electroplating and of the bumps were evaluated. The result can be summarized as follows.

Electroplating rate increased with increasing current density, and the rate was 0.25 and 2.7 μm/min at 1 and 8 A/dm^2, respectively. Electroplated Sn–Cu alloy kept almost constant composition of Sn–(0.9–1.4%)Cu in the range of current density between 1 and 8 A/dm^2. The electroplating condition of 5 A/dm^2 (current density) and 2 h (plating time) gave optimal size of mushroom bump as 120-μm column diameter and 75-μm bump height. The mushroom bump changed to hemispherical with 140-μm diameter by air reflow. The partly nonuniformity of

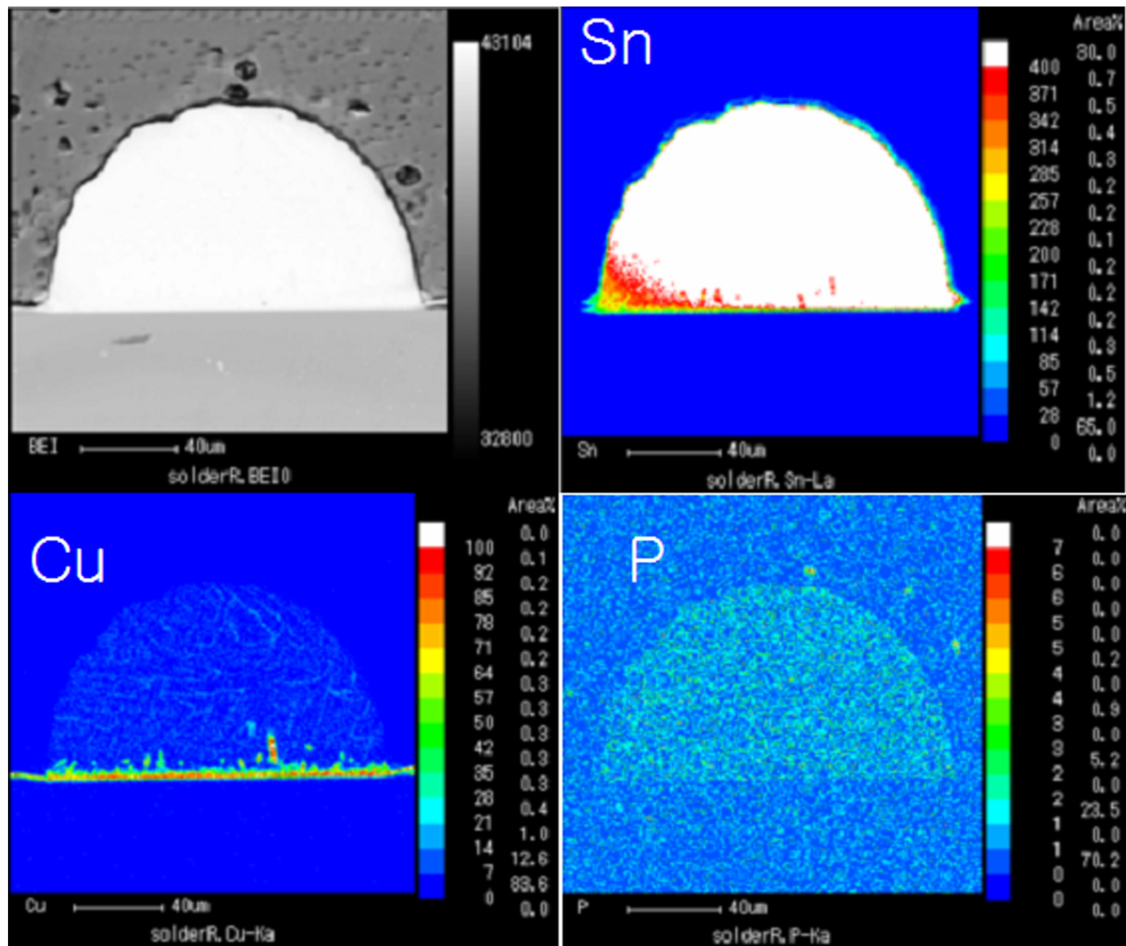

Fig. 10. Analysis of element distribution by EPMA mapping on the reflowed Sn–Cu solder bump. (Color version available online at http://ieeexplore.ieee.org.)

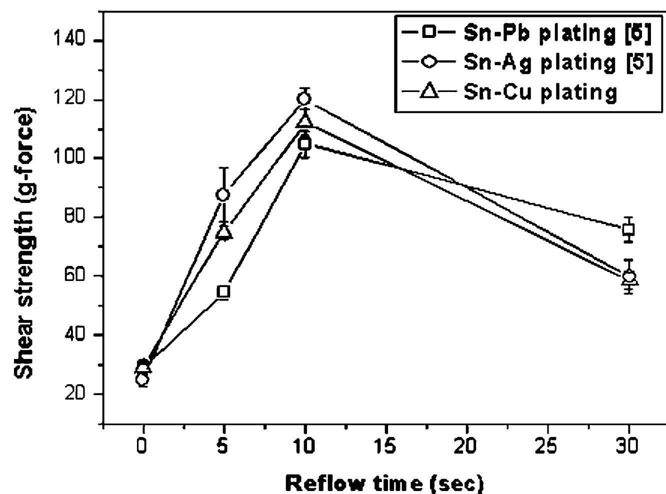

Fig. 11. Shear bond strength of hemispherical solder bumps with reflow time.

chemical composition in mushroom bump was mostly homogenized in hemispherical bump by air reflow. The shear bond strength of the Sn–Cu hemispherical bump showed 113 gf by reflowing at 260 °C for 10 s. The electroplated Sn–Cu was estimated to have a good consequence in both of bump shape and bond strength.

References

[1] M. R. Harrison, J. H. Vincent, and H. A. H. Steen, "Lead-free reflow soldering for electronics assembly," *Soldering Surface Mount Technol.*, vol. 13, no. 3, pp. 21–38, 2001.

[2] K. Suganuma, "Advances in lead-free electronics soldering," *Curr. Opin. Solis State Mater. Sci.*, vol. 5, no. 1, pp. 55–64, 2001.

[3] J. H. Lau and S. W. R. Lee, *Chip Scale Package*. New York: McGraw-Hill, 1999, p. 80.

[4] S. M. Hong, J. P. Jung, and C. S. Kang, "Flux-free direct chip attachment of solder-bump flip chip by Ar + H_2 plasma treatment," *J. Electron. Mater.*, vol. 31, no. 10, pp. 1104–1111, 2002.

[5] H. Hwang, S. M. Hong, J. P. Jung, and C. S. Kang, "Pb-free solder bumping for flip chip package by electroplating," *Soldering Surf. Mount Technol.*, vol. 15, no. 2, pp. 10–16, 2003.

[6] S. A. Merrit, P. J. S. Heim, S. H. Cho, and M. Dagenais, "Controlled solder interdiffusion for high power semiconductor laser diode die bonding," *IEEE Trans. Compon., Packag. Manuf. Technol. B*, vol. 20, no. 2, pp. 141–145, May 1997.

[7] S. M. Hong, C. S. Kang, and J. P. Jung, "Fluxless Sn-3.5 mass%Ag solder bump flip chip bonding by ultra-sonic wave," *Mater. Trans.*, vol. 43, no. 6, pp. 1336–1340, 2002.

[8] B. Djurfors and D. G. Ivey, "Microstructural characterization of pulsed electrodeposited Au/Sn alloy thin films," *Materi. Sci. Eng. B (Switzerland)*, vol. B90, no. 3, pp. 309–320, 2002.

[9] G. Holmbom, J. A. Abys, H. K. Straschil, and M. Svensson, "Electrodeposition, growth morphology and melting characteristics of gold-tin eutectic alloys," *Plating Surface Finishing*, pp. 66–73, Apr. 1998.

[10] M. Fukuda, K. Imayoshi, and Y. Matsumoto, "Effects of thiourea and polyoxyethylene lauryl ether on electrodeposition of Sn–Ag–Cu alloy as a Pb-free solder," *J. Electrochem. Soc.*, vol. 149, no. 5, pp. C244–C249, 2002.

[11] S. Arai and T. Watanabe, "Microstructure of Sn–Ag alloys electrodeposited from pyrophosphate-iodide solutions," *Mater. Trans., JIM*, vol. 39, no. 4, pp. 439–445, 1998.

[12] M. Li, F. Zhang, W. T. Chen, K. Zeng, K. N. Tu, H. Balkan, and P. Elenius, "Interfacial microstructure evolution between eutectic SnAgCu solder and Al/Ni(V)/Cu thin films," *J. Mater. Res. (USA)*, vol. 17, no. 7, pp. 1612–1621, Jul. 2002.

[13] S. Chada, R. A. Fournelle, W. Laub, and D. Shangguan, "Copper substrate dissolution in eutectic Sn–Ag solder and its effect on microstructure," *J. Electron. Mater.*, vol. 29, no. 10, pp. 1214–1221, 2000.

[14] K. S. Bae and S. J. Kim, "Microstructure and adhesion properties of Sn-0.7 Cu/Cu solder joints," *J. Mater. Res.*, vol. 17, no. 4, pp. 743–746, 2002.

[15] M. Fukuda, K. Hirakawa, and Y. Matsumoto, "Sn–Cu alloy electrodeposition for lead-free solder," *Hyomen Gijutsu (J. Surface Finishing Soc. Japan)*, vol. 50, no. 12, pp. 1125–1129, 1999.

[16] S. Arai, Y. Funaoka, N. Kaneko, and N. Shinohara, "Electrodeposition of Sn–Cu alloy from phosphate bath," *Electrochem.*, vol. 69, no. 5, pp. 319–323, 2001.

[17] J. H. Kim, M. S. Suh, and H. S. Kwon, "Effects of plating conditions on the microstructure of 80 Sn-20 Pb electrodeposits from an organic sulphonate bath," *Surface Coating Technol.*, vol. 78, pp. 56–63, 1996.

[18] A. C. Tan, *Tin and Solder Plating in the Semiconductor Industry*. London, U.K.: Chapman & Hall, 1993, p. 27.

[19] M. Carano, "Tin-lead plating," *Plating Surface Finishing*, pp. 44–45, Aug. 2003.

[20] A. C. Tan, *Tin and Solder Plating in the Semiconductor Industry*. London, U.K.: Chapman & Hall, 1993, p. 240.

[21] J. L. Puippe and W. Fluehmann, "Electrodepostion and properties of a silver-tin alloy," *Plat. Surface Finishing*, vol. 70, no. 1, pp. 46–48, 1983.

[22] Y. J. Tan and K. Y. Lim, "Understanding and improving the uniformity of electrodeposition," *Surface Coating Technol.*, vol. 167, pp. 255–262, 2003.

Seok Won Jung received the B.S. and M.S. degrees from the Department of Materials Science and Engineering, University of Seoul, Seoul, Korea, in 2001 and 2003, respectively.

He is currently in the military service as a first lieutenant. His research interest is in the field of electroplating and soldering for electronics packaging.

Jae Pil Jung received the B.S. and Ph.D. degrees from the Department of Metallurgical Engineering, Seoul National University, Seoul, Korea, and the M.S. degree from the Department of Materials Science and Engineering, Korea Advanced Institute of Science and Technology, Daejeon, Korea.

He was a Senior Researcher at the Department of Welding and Joining, Korea Institute of Machinery and Metals, for 12 years. He is currently a Professor at the Department of Materials Science and Engineering, University of Seoul, where he has been since 1996. He holds the Chair in the Microjoining and Packaging Committee of KWS. His research interests lie in the areas of interconnection materials and processes for electronics including soldering, wire bonding, and other microjoining processes and mechanics of electronics packaging.

Y. (Norman) Zhou received the B.A.Sc. and M.A.Sc. degrees from the Department of Mechanical Engineering, Tsinghua University, Beijing, China, and the Ph.D. degree from the Department of Metallurgy and Materials Science, University of Toronto, Toronto, ON, Canada.

He was a Lecturer in the Department of Mechanical Engineering, Tsinghua University, and a Materials Scientist in the Fuel Development Branch, Atomic Energy of Canada, Ltd, Chalk River, Ontario, Canada. He also was a Senior Research Engineer at the Microjoining and Plastics Group, Edison Welding Institute, Columbus, OH. He is currently an Associate Professor in the Department of Mechanical Engineering, University of Waterloo (www.me.uwaterloo.ca/dept/zhou.html). He has more than 20 years industrial, teaching, and research experience in materials joining technologies. His current research interests are in the field of microjoining (wire bonding, resistance and laser microwelding, brazing and soldering, etc.).

Dr. Zhou is currently a holder of the Canada Research Chair in Microjoining (www.chairs.gc.ca).